

Non-Volatile Resistive Memory Characteristics in TiO_x based simple Metal-Insulator-Metal Structure

Debjoyti Banerjee,^a Soumi Mukherjee,^a Rajeswar Panja^{a,*}

^aDepartment of physics, Techno India University, West Bengal, Kolkata-700091, India

Abstract

Low power and space consumption are two essential criteria for future non – volatile memory technology. Among other emerging memory technologies resistive memory becomes very promising and efficient one because it fulfills all criteria for sustainable memory technology. In this work we have investigated the resistive switching characteristics in FTO/ TiO_x /Metal structure. The device shows low power switching characteristics at $\pm 2\text{V}$ with current of $2.7 \mu\text{A}$. The device shows unique properties of bipolar resistive switching. The high resistance ratio of $>10^2$ and uniform switching cycles are another potential factors of this structure. We have also investigated the current conduction mechanism for the HRS and LRS of our device during SET and RESET processes.

Keywords: Resistive switching, RRAM, TiO_2 , memory technology

1. Introduction

At present, resistive random access memory (RRAM) becomes very promising candidate for future non-volatile memory technology because of its simple capacitor like structure, low space consumption, cost-effectiveness nature.[1-3]. Basically, a dielectric medium like HfO_2 , Ta_2O_5 , Al_2O_3 , TiO_2 etc.as a switching medium is sandwiched between two metal electrodes [4-8]. The set and reset processes are the result of conductive filament formation and rupture inside the switching medium, respectively [9]. For sustainable and efficient performance of a device the selection of switching medium is very important. Switching medium must have wide band gap, stability for large cycle operation and retentivity. In this regard, titanium dioxide (TiO_2) is highly important in both theoretical and experimental field of research because of its very interesting electronic structures and wide band gap (3.23eV for anatase) which can be tuned by several processes [10]. At a lower synthesis temperature (600 °C), TiO_2 nanoparticle tends to nucleate to an anatase phase as surface Gibbs free

energy is lower for anatase phase than the rutile. Physical properties of TiO_2 not only depend on the phase structure but it depends also on the agglomerated micro structure, pores, and particle size. For different physical and chemical process like charge transfer, chemical reaction, photon absorption etc. the molecules on the surface of a particles are more active than those stay inside. Hence, surface property is very important for device performance.

We can deposit titanium oxide using different deposition processes like sputter, thermal evaporation, e-beam evaporation, sol-gel etc. on various substrates. In this work we have used sol-gel with spin coating techniques for TiO_x thin film for the simplicity of the technique and easy to prepare in laboratory. There are several promising reports on TiO_2 based resistive memory characteristics on different research work. C.Yoshida *et al.* fabricated a device with structure Pt/ TiO_2 /TiN/Pt/Ti/ SiO_2 /Si, with set and reset

voltages -1.1V and 0.7V, respectively and the resistance ratio is 10^2 [11]. Chanwoo Lee *et al.* designed a Ti/TiO₂/W device with unipolar switching having set and reset voltages 1.4V and 0.6V, respectively. The device shows resistance ratio $>10^4$ - 10^5 and the retention is $>10^4$ s [12]. H.Y.Jeong fabricated a Al/TiO₂/Al/PES device with set and reset voltages -2V and -1.8V, respectively and the resistance ratio 10 [13]. M.Yanget *al.* fabricated a device with structure ITO/TiO₂/ITO/glass with set and reset voltages 2.3V and -2.5V, respectively [14]. H.Y.Jeong *et al.* fabricated a device with structure Al/a-TiO₂/Al/SiO₂/Si with set and reset voltages -2.2V and 2.2V, respectively [15]. Kuyyadi P Bijuet *al.* fabricated a device with bipolar switching of structure Pt/TiO₂/W with set and reset voltages +20V and -20V, respectively. This device showed resistance ratio and endurance of 10 and 10^3 respectively [16]. A.Regoutzet *al.* fabricated a device

2. Device Fabrication

For the preparation of titanium oxide thin film, we have used Titanium (IV) Isopropoxide or TTIP (sigma-Aldrich) precursor. At first, we have mixed 1.5 ml of TTIP with 20 ml of Ethanol (99.5 %). This creates a white sol solution. Then we put the solution on a magnetic stirrer for stirring along with a magnetic bit. After that, we have added acetic acid dropwise with the help of a microtip pipette, until the solution became colourless. Thus, after addition of 1 ml of acetic acid, the solution became colourless and a gel like solution was formed. After that, we have left the solution for 1 day for aging. Then, we have taken a FTO coated glass (Sigma – Aldrich) and cleaned it with soap water then deionised water and after that with acetone

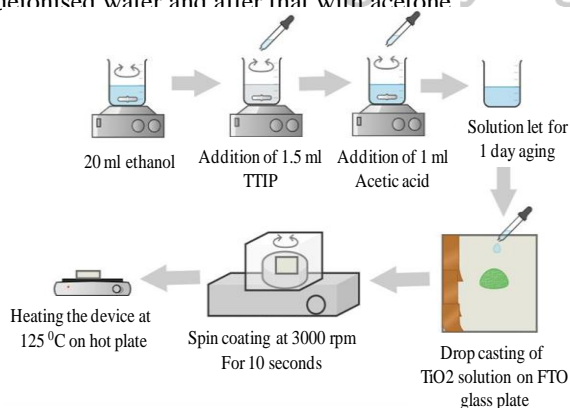


Fig 1: Schematic diagram of the fabrication of TiO_x thin film on FTO glass plate.

Then, we have covered a portion of FTO coated glass with Crypton tape so that by removing the tape we can get the bottom contact from FTO, and put it on a spin coater (EZspin – ADV – Apex instrument). Then, we have poured the sol-gel solution of TiO₂ on FTO coated glass with the help of a microtip pipette. Then

with structure Pt/TiO₂/Pt/Ti/SiO₂/Si with set and reset voltages -2.2V and 1.6V, respectively [17]. M.Xiaet *al.* fabricated a device with structure Al/TiO₂ NRA/TiO₂ seed/FTO device with set and reset voltages 4V and -4V, respectively [18]. S.Royet *al.* fabricated a device showing bipolar switching with structure Al/TiO₂/Si MOS with set and reset voltages +2.8V and -3V, respectively [19]. Shi-Xiang Chen *et al.* fabricated a device of structure ITO/TiO₂/Pt/Ti with set and reset voltages 0.6V and -0.5V. They showed resistance ratio and retention of 10^1 and 10^2 , respectively [20]. In this research work we have demonstrated low power switching characteristics of $< \pm 2$ V set/ reset voltages with $< 2.7 \mu\text{A}$ current in the simple FTO/ TiO_x/Metal structure. The device shows > 50 consecutive, uniform switching cycles with resistance ratio $> 10^2$. These characteristics of our device make it as a potential candidate for future memory technology

we have made spin for the preparation of the thin film for 3000 rpm for 10 s. After that we have put the device on a heater with 125° temperature for 15 minutes. So that the film gets dry. The complete processes is step wise schematically shown in Fig. 1. The current –voltage (I -V) characteristics of our FTO/TiO_x/ metal structure are measured using Keithley sourcemeter 2400.

3. Result and discussions

3.1 Current – voltage (I-V) characteristics

The bipolar resistive switching I-V characteristics at a low current of $< 2.7 \mu\text{A}$ for the FTO/TiO_x/Metal device are shown in the Fig. 2. The device shows formation free switching cycles. The arrows (1 → 4) indicate the direction of I-V sweep as (0 → +2 → 0 → -2 → 0). Therefore, low operation voltage of $< 2\text{V}$ and -2V is observed. The reset current is less than 0.2 nA, the set current is about 2.7 μA . We have set the compliance current is about 1mA to avoid any destruction of our device. The currents at HRS and LRS are $\sim 1.7\text{nA}$ and $\sim 7.8 \mu\text{A}$ at read voltage, $V_{\text{read}} = -1\text{V}$ in RESET state. In SET state the currents at HRS and LRS are $\sim 13 \text{nA}$ and $\sim 1.1\mu\text{A}$ at $V_{\text{read}} = 0.6 \text{V}$ in SET state. We have taken two different read voltages in reset and set state to indicate the efficient performance zone of our bipolar device. The resistance ratio $s > 10^2$.

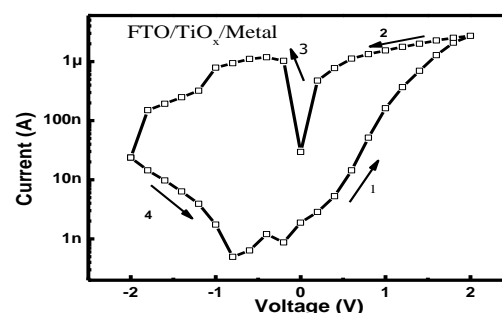


Fig 2: Current – voltage characteristics of FTO/TiO_x/metal structure

The device shows consecutive > 50 uniform switching cycles. The sweeping voltages are (0 → +2 → 0 → -2 → 0) applied on the top electrode with respect to the grounded bottom electrode is shown through arrows from 1 to 4 in the Fig. 3. A current compliance of 1 mA is applied to avoid any damage of the device.

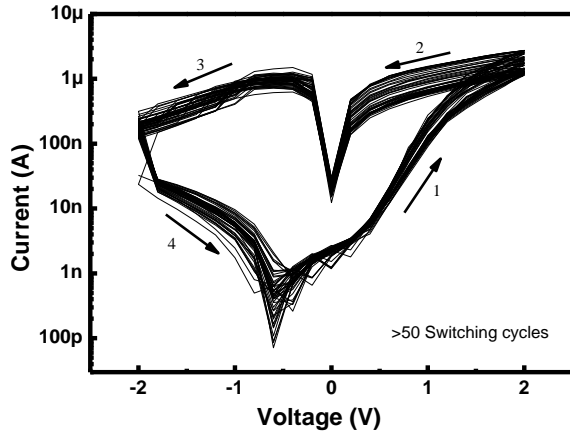


Fig 3: Consecutive 50 uniform switching cycles shows the robustness of the device

3.2 Cumulative probability

The Fig. 4 shows the statistical distribution of current at low resistance state (LRS) and high resistance state (HRS) for 50 numbers of switching cycles. The V_{read} values are -1V and 0.6V for reset and set state, respectively. The cycle-to-cycle uniformity is clearly seen from cumulative probability plot. The HRS/LRS ratio was obtained $>10^2$.

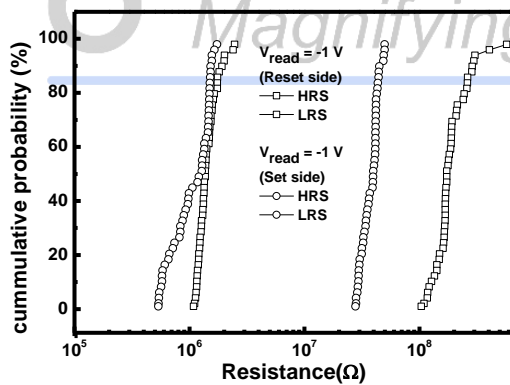


Fig 4: Cumulative probability plot of current at HRS/LRS for reset and set side.

3.3 Current Conduction mechanisms

We have investigated about the possible current conduction mechanism for both HRS and LRS in reset state of our device. We have focused on the reset zone because this shows the effective memory characteristics compare to set zone. After verifying different conduction mechanisms such as Schottky, Poole – Frenkel (PF), Ohmic etc. it is observed that the HRS of the device follows Schottky conduction

whereas the LRS follows the Ohmic conduction. This is shown in Fig. 5. All the data are taken at room

temperature. Since the reset of our device is a result of negative bias on the top electrode with respect to the bottom electrode, hence the possibility of filament rupture is at the TiO_x/FTO interface. At that interface electric field becomes very high and as a result filament rupture and formation highly favourable there. So, there is a Schottky barrier at the TiO_x/FTO interface. This filament formation and rupture processes has been explained explicitly in next paragraph. On the other hand the Ohmic conduction in LRS indicates the formation of Ohmic path inside the device during set process.

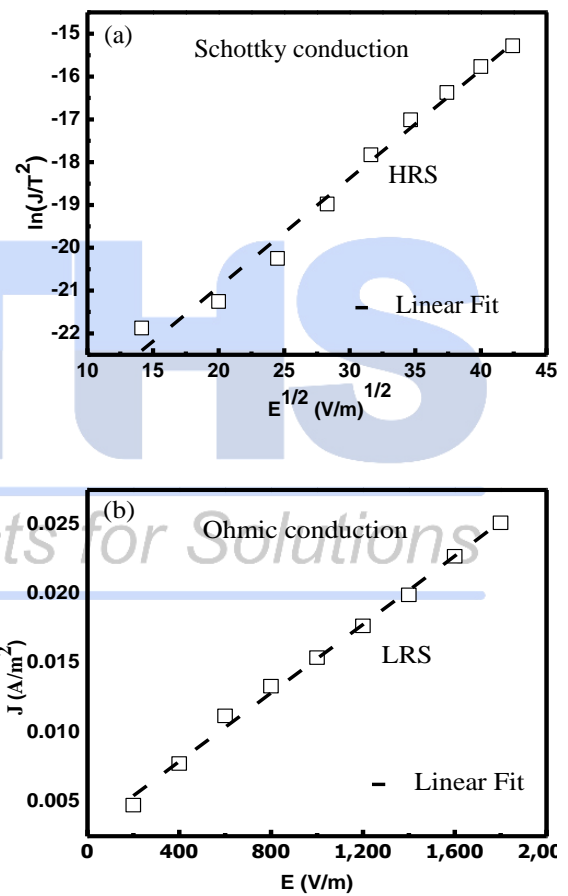


Fig 5: Current conduction mechanism shows (a) Schottky conduction at the HRS and (b) Ohmic conduction at the LRS of the device.

To verify the Schottky conduction we have used the following relation [21].

$$J = A^*T^2 \exp\left(\frac{-q\left(\phi_B - \sqrt{\frac{qE}{4\pi\epsilon_0\epsilon_r}}\right)}{KT}\right)$$

Where J is the current density, A^* is the effective Richardson constant, K is the Boltzmann's constant, T is the absolute temperature, q is the electronic charge,

$q\phi_B$ is the Schottky barrier height (i.e., conduction band offset), E is the electric field across the dielectric, ϵ_0 is the permittivity of the free space and ϵ_r is the dynamic dielectric constant. On the other hand for the verification of Ohmic conduction we have used the following equation [21].

$$J = q\mu E N_c \exp\left(-\frac{E_g}{2kT}\right)$$

Where, J is the current density, μ is the electron mobility, N_c is the effective density of states of the conduction band, E_g is the energy band gap. Further high temperature study for conduction mechanism is needed.

4. Conclusion

The resistive random access memory becomes very promising and efficient candidate for future memory technology for its simple structure, low power consumption and cost – effectiveness. In this study we have found out the low power memory characteristics in our structure FTO/TiO_x/metal structure. The device shows uniform > 50 switching cycles at low current of < 2.7 μ A. The device also shows the formation free set/reset characteristics at the low operating voltages of +/- 2 V. This low power consumption and uniformity of our TiO_x based device makes it very promising for future non - volatile memory applications. We have also seen that the probable current conduction mechanisms in HRS follows Schottky conduction and LRS follows Ohmic conduction and which are compatible with filamentary switching phenomena.

Acknowledgements

This work was supported by Techno India University, West Bengal. The authors are also grateful to department of physics, Techno India University, West Bengal for their experimental support.

References

- [1] Prakash, A., Jana, D., & Maikap, S. (2013). TaO_x-based resistive switching memories: prospective and challenges. *Nanoscale research letters*, 8, 1-17.
- [2] Yang, J. J., Strukov, D. B., & Stewart, D. R. (2013). Memristive devices for computing. *Nature nanotechnology*, 8, 13-24.
- [3] F. Pan, S. Gao, C. Chen, C. Song, F. Zeng, Mater. Sci. Eng. Rep. 83 (2014) 1–59.
- [4] Lee, M. J., Lee, C. B., Lee, D., Lee, S. R., Chang, M., Hur, J. H., ... & Kim, K. (2011). A fast, high-endurance and scalable non-volatile memory device made from asymmetric Ta₂O₅-x/TaO₂-x bilayer structures. *Nature materials*, 10(8), 625-630.
- [5] Rahaman, S. Z., Lin, Y. D., Lee, H. Y., Chen, Y. S., Chen, P. S., Chen, W. S., ... & Wang, P. H. (2017). The role of Ti buffer layer thickness on the resistive switching properties of hafnium oxide-based resistive switching memories. *Langmuir*, 33(19), 4654-4665.
- [6] Celano, U., Goux, L., Belmonte, A., Opsomer, K., Franquet, A., Schulze, A., ... & Vandervorst, W. (2014).
- [7] Three-dimensional observation of the conductive filament in nanoscaled resistive memory devices. *Nano letters*, 14(5), 2401-2406.
- [8] Panda, D., Dhar, A., & Ray, S. K. (2011). Nonvolatile Memristive Switching Characteristics of TiO₂ Embedded With Nickel Nanocrystals. *IEEE transactions on nanotechnology*, 11(1), 51-55.
- [9] Park, T. H., Song, S. J., Kim, H. J., Kim, S. G., Chung, S., Kim, B. Y., ... & Hwang, C. S. (2015). Thickness-dependent electroforming behavior of ultra-thin Ta₂O₅ resistance switching layer. *physica status solidi (RRL)–Rapid Research Letters*, 9(6), 362-365.
- [10] Valov, I., Waser, R., Jameson, J. R., & Kozicki, M. N. (2011). Electrochemical metallization memories—fundamentals, applications, prospects. *Nanotechnology*, 22(25), 254003.
- [11] M. H. Mithun, A. Sayed, I. Rahaman, PETI 19 (2021) 45 -52.
- [12] Yoshida, C., Tsunoda, K., Noshiro, H., & Sugiyama, Y. (2007). High speed resistive switching in Pt/TiO₂/TiN film for nonvolatile memory application. *Applied Physics Letters*, 91(22).
- [13] Lee, C., Kim, I., Choi, W., Shin, H., & Cho, J. (2009). Resistive switching memory devices composed of binary transition metal oxides using sol-gel chemistry. *Langmuir*, 25(8), 4274-4278.
- [14] Jeong, H. Y., Kim, Y. I., Lee, J. Y., & Choi, S. Y. (2010). A low-temperature-grown TiO₂-based device for the flexible stacked RRAM application. *Nanotechnology*, 21(11), 115203.
- [15] Yang, M., Pei-Jian, Z., Zi-Yu, L., Zhao-Liang, L., Xin-Yu, P., Xue-Jin, L., ... & Dong-Min, C. (2010). Enhanced resistance switching stability of transparent ITO/TiO₂/ITO sandwiches. *Chinese Physics B*, 19(3), 037304.
- [16] Jeong, H. Y., Kim, S. K., Lee, J. Y., & Choi, S. Y. (2011). Role of interface reaction on resistive switching of metal/amorphous TiO₂/Al RRAM devices. *Journal of The Electrochemical Society*, 158(10), H979.
- [17] Biju, K. P., Liu, X., Shin, J., Kim, I., Jung, S., Siddik, M., ... & Hwang, H. (2011). Highly asymmetric bipolar resistive switching in solution-processed Pt/TiO₂/W devices for cross-point application. *Current Applied Physics*, 11(4), S102-S106.
- [18] Regoutz, A., Gupta, I., Serb, A., Khiat, A., Borgatti, F., Lee, T. L., ... & Prodromakis, T. (2016). Role and optimization of the active oxide layer in TiO₂-based RRAM. *Advanced Functional Materials*, 26(4), 507-513.
- [19] Xiao, M., Musselman, K. P., Duley, W. W., & Zhou, Y. N. (2017). Reliable and low-power multilevel resistive switching in TiO₂ nanorod arrays structured with a TiO_x seed layer. *ACS Applied Materials & Interfaces*, 9(5), 4808-4817.
- [20] Roy, S., Tripathy, N., Pradhan, D., Sahu, P. K., & Kar, J. P. (2018). Electrical characteristics of dip coated TiO₂ thin films with various withdrawal speeds for resistive switching applications. *Applied Surface Science*, 449, 181-185.
- [21] Chen, S. X., Chang, S. P., Chang, S. J., Hsieh, W. K., & Lin, C. H. (2018). Highly stable ultrathin TiO₂ based resistive random access memory with low operation voltage. *ECS Journal of Solid State Science and Technology*, 7(7), Q3183.
- [22] F. C. Chiu, Adv. Mater. Sci. Eng., 2014 (2014) 1-18.